


REVIEW

Open Access



3D bioprinting of collagen-based materials for oral medicine

Bosen Yang^{1†}, Hai Liu^{1†}, Linli Jiang², Yiwei Zeng², Yiyuan Han^{3*}, Chuanlu Sha¹, Xin Xie¹, Hui Li^{2*}, Jiajing Zhou^{1*}  and Wei Lin¹

Abstract

Oral diseases have emerged as one of the leading public health challenges globally. Although the existing clinical modalities for restoration of dental tissue loss and craniomaxillofacial injuries can achieve satisfactory therapeutic results, they cannot fully restore the original complex anatomical structure and physiological function of the tissue. 3D printing of biological tissues has gained growing interest in the field of oral medicine with the ability to control the bioink component and printing structure for spatially heterogeneous repairing constructs, holding enormous promise for the precise treatment of oral disease. Particularly, collagen-based materials have been recognized as promising biogenic bioinks for the regeneration of several tissues with high cell-activating and biocompatible properties. In this review, we summarize 3D printing methods for collagen-based biomaterials and their mechanisms. Additionally, we highlight the animal sources of collagen and their characteristics, as well as the methods of collagen extraction. Furthermore, this review provides an overview of the 3D bioprinting technology for the regeneration of the pulpal nerve and blood vessels, cartilage, and periodontal tissue. We envision that this technique opens up immense opportunities over the conventional ones, with high replicability and customized function, which can ultimately promote effective oral tissue regeneration.

Keywords 3D bioprinting, Oral medicine, Tissue engineering, Collagen, Scaffold materials, Bioink, Hydrogel

[†]Bosen Yang and Hai Liu contributed equally to this work.

*Correspondence:

Yiyuan Han

Yiyuan.Han@childrens.harvard.edu

Hui Li

drlihui@outlook.com

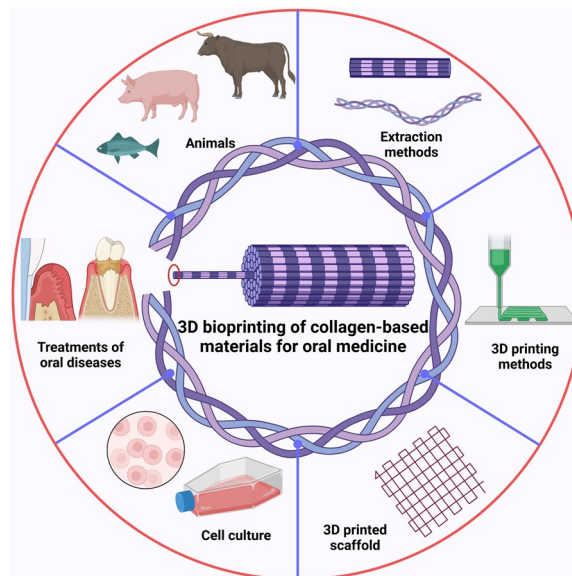
Jiajing Zhou

jjzhou@scu.edu.cn

Full list of author information is available at the end of the article



Graphical Abstract



1 Introduction

Oral health is important to the overall health and well-being of the public. According to the Global Burden of Disease (GBD) 2015 study, nearly 3.5 billion people worldwide have suffered from pain and discomfort associated with oral disease [1], including dental caries, periodontal disease, craniomaxillofacial tissues damage, etc. For example, dental caries, the most prevalent one, caused by an ecological disorder of the dental biofilm adhering to the surface of tooth enamel [2], can spread to the pulp and cause infection, resulting in severe pain [3]. Periodontal disease is a long-term inflammatory disease that affect tissues surrounding and supporting the teeth, usually caused by trauma or bacterial infection. The injury of periodontal tissues (e.g., gums, periodontal ligaments, dental bone, alveolar bone and other supporting periodontal connective tissues) is a hallmark of these diseases [4–6]. The ultimate goal of oral treatment is to regenerate the original structure and performance of the periodontal complex [7]. However, it is still challenging to realize the recovery of these tissue injuries. Although the existing clinical modalities have shown promising therapeutic efficacy in the restoration of dental tissue loss and craniomaxillofacial injuries, they still cannot restore the original complex anatomical structure and physiological function of the tissue.

Three-dimensional (3D) bioprinting has attracted immense interest in the field of biomedical engineering due to the desire for precision and customization in

tissue regeneration. This technique, first used by Charles Hull in 1986, employed layered light-cured materials to form a 3D structure in sequence [8]. Specifically, a digital model file is used as the basis for constructing an object in progressive layers utilizing a bondable material master such as powdered metal or plastic. It can directly produce components of virtually any shapes on the basis of the computer graphics data, eliminating the need for complicate processing, significantly shortening product development cycles, lowering production costs, and enhancing product functions [9]. Over the past decade, 3D bioprinting technology has been widely applied in medical fields including regeneration medicine [10], anatomical model construction [11], pharmaceutical formulations [12, 13]. As a result of this technology's potential to build 3D bionic functional tissues, it has gradually been applied to the field of dentistry to precisely target oral tissue regeneration and repair of craniomaxillofacial injuries. Dental surgery has evolved from a conventional, purely empirical approach to digitalization and precision owing to the usage of 3D printing technologies.

The first case of a large periodontal osseous defect being treated in a human using 3D-printed technology was reported by Rasperini et al. [14]. A bioresorbable patient-specific polymer scaffold was designed with signaling growth factor and the treated area underwent good recovery for 12 months during the therapy. This work revealed that 3D-printed image-based scaffolds provide the potential for reconstruction of oral tissues.

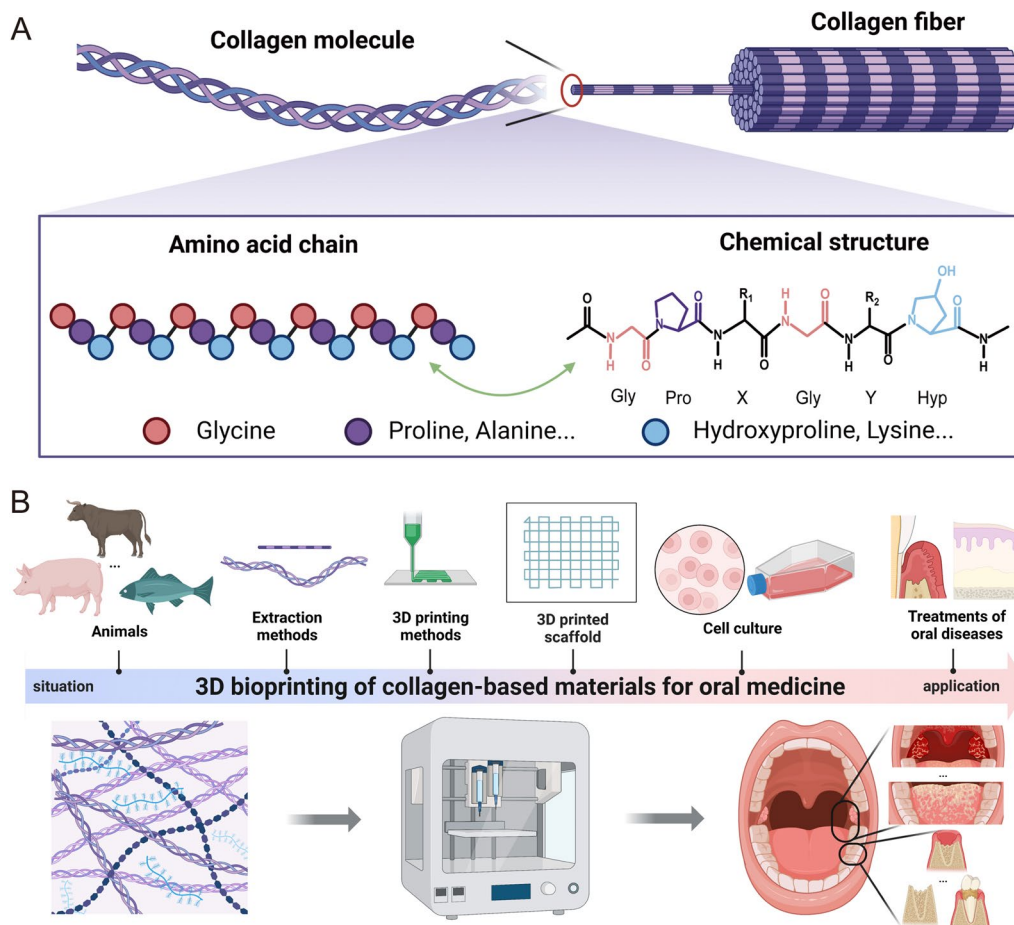


Fig. 1 A Collagen amino acid chain. B 3D bioprinting of collagen-based materials for oral medicine

Employing 3D bioprinting to create scaffolds, tissue analogs, and organs is an innovative solution that can help dentists overcome some of the most pressing problems today [15]. Some scholars have demonstrated that the application of 3D printing technology improves operational accuracy by 36.23% and shortens the operational time by 17.63% [16, 17]. For example, the construction of 3D printed scaffolds that allow cell attachment, migration, and proliferation, has been exploited, particularly for the regeneration of complex anatomical structure (e.g., pulpodentinal complex, periodontal tissue complexes) [18–20]. The development of 3D printing technology has catalyzed significant advances in the field of regenerative dentistry.

Collagen is a main component of the extracellular matrix, and therefore has widespread use for tissue engineering. It has also been extensively tested in dental regeneration studies due to its structural and chemical similarity to the main structural proteins comprising the extracellular matrix of oral tissues [21]. This superfamily of proteins is featured by the repeating amino acid

motifs (Gly–X–Y) in each chain, in which X represents two amino acids (e.g., proline or hydroxyproline) and Y refers to any amino acids (Fig. 1A). The collagen molecule is comprised of a triple helical region where three amino acid chains self-aggregate to form a right-handed helix structure, and two nonhelical regions at either end of the helix, which define the structural element of all collagens [22, 23]. The triple helix possesses the glycine in the interior of the helix, while X and Y are exposed to the exterior [14]. The arginine-glycine-aspartate sequence in collagen can interact with cells, and the resulting 3D collagen scaffolds can promote cell adhesion, proliferation, and differentiation [24]. Particularly, cells can uptake these degraded collagen scaffolds, which further facilitate the development of new tissue [25]. However, pure collagen lacks certain mechanical properties and degrades rapidly when used as tissue scaffolds in living organisms. To this end, collagen is often engineered with other materials to create reliable constructs with desirable functions.

In this review, we summarize 3D printing techniques for collagen-based biomaterials and their design

rationales for oral medicine. These techniques offer advantages over the conventional ones, and demonstrate the competence to create reproducible, bespoke, and functionalized structures that can effectively facilitate the regeneration of different tissues. The animal sources of collagen and extraction strategies for collagen is also compared. We further highlight advances in 3D bioprinting collagen-based materials used in oral medicine, with a particular emphasis on the pulpal nerve and blood vessels, cartilage, and periodontal tissue. Finally, we outline the challenges that must be overcome to translate 3D bioprinting technology in clinic medicine (Fig. 1B). We envision the combination of collagen and 3D printing technology will create spatially functional materials to drive the advance of oral medicine.

2 Extraction methods for collagen

Collagen is a natural high molecular protein and an important renewable resource, which is commonly found in the skin, cartilage, and other connective tissues of animals, and makes up 25–30% of all biological proteins [26–28]. Collagen possesses outstanding biological properties (e.g., low immunogenicity and high biodegradability) and physical characteristics (e.g., high flexibility, strong mechanical strength, stable structural stability, and satisfactory permeability) [29–31]. Thus, it has an irreplaceable role in many fields, such as biomedicine (e.g., hemostasis [32], antibacterial [33], tissue engineering [34], drug release [35, 36]), food [37, 38], cosmetics [39–41] and engineering applications [42–46]. With increasing interest and demand of collagen, collagen sources and extraction methods are extensively explored. The common methods of collagen extraction are alkali extraction [47], acid extraction [48], hot water extraction [49], enzyme extraction [50] and other extraction methods [51], which will be briefly introduced below.

2.1 Collagen sources from animals

Collagen sources can be obtained from animal sources, human tissues, and recombinant genetic techniques (Fig. 2). For animal sources, bovine, porcine [52], rat (e.g., tail tendon [53]), and marine animals (e.g., fish [54]) are the most used species. Specifically, cowhide has roughly 30% protein content, and collagen is mainly present in the inner corium layer [55]. Collagen is also the main protein (over 90%) in bovine bone, which has a good capacity to scavenge free radicals and inhibit the oxidation of polyunsaturated fatty acids in cells [56]. The structure of pig skin is more similar to that of human skin tissue [57], and thus is beneficial for human absorption, which is often processed into moisturizing dressings for cosmetic purposes. Rat tail tendon (RTT) is one of the most common sources of type I collagen used by researchers, leading to

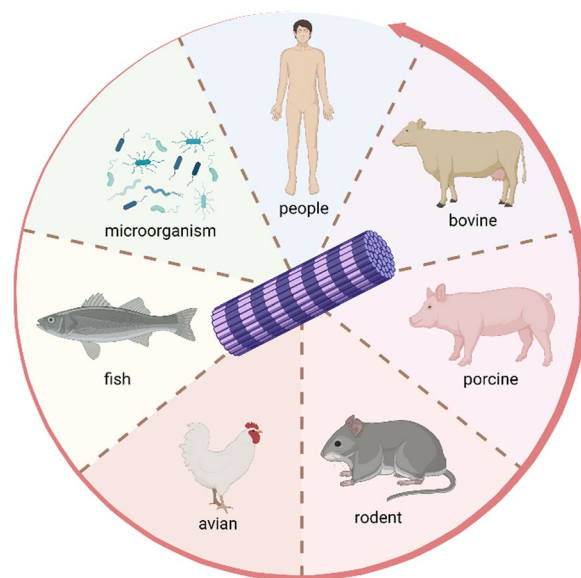


Fig. 2 Diverse sources of collagen

various protocols for type I collagen isolation and characterization. RTT contains 90–95% type I collagen by weight, and the high percentage of collagen ensures a high yield after isolation [58]. These sources are cheap and easily available, but they frequently develop allergies and misfolds, causing several diseases such as bovine spongiform encephalopathy [59]. To this end, type I collagen derived from marine sources has gained attention over the past decade, and has shown advantages such as the reduced risk of disease transmission. However, marine collagen including those from fish skin, bone and fins denatures has a more variable composition and a lower denaturation temperature ($\sim 27^\circ\text{C}$) in comparison to mammalian collagen ($\sim 40^\circ\text{C}$), which may limit its usage in biomedical applications [60].

2.2 Alkali extraction

The alkali extraction method uses alkaline compounds (e.g., NaOH , Na_2CO_3) to destabilize the amino acids containing hydroxyl and hydrophobic groups in collagen. The operation of alkali extraction is simple (e.g., soaking, rinsing, suspending, heating, and centrifuging in alkali), but the molecular mass of obtained collagen is relatively low and the yield of collagen is poor. Prolonged extraction will lead to the destruction of the three-stranded helix structure, cleaved amide bonds, and oxidized amino acids (e.g., cysteine, serine, threonine and tyrosine containing sulfur and hydroxyl groups). Particularly, this extraction method may produce D-type amino acids that are cancerigenic and mutagenic. Therefore, in order to extract native collagen with high content, the alkali extraction is

Table 1 Comparison of different extraction methods

Methods	Resources	Conditions	Yields/%	Pros	Cons
Alkali extraction	Tendon of Yezo sika deer [62]	0.1 M NaOH, 48 h	41.8	Simple operation	Toxic D-amino acids may be produced; difficult control on reaction
	Squid skins [63]	pH 11.5 NaOH solution, 24 h	90		
Acid extraction	Sailfish skin [64]	0.5 M acetic acid, 4 °C, 72 h	5.76	Preserved collagen structure	Lower extraction rate; equipment corrosion; heavy pollution
	Tissue of Chinese soft-shelled turtle [65]	0.5 M acetic acid, 1:10 (w/v), 48 h	1.0		
Hot water extraction	Fish skin [66]	150–250 °C, 350–3900 kPa	4.8–7.0	Easy, non-toxic	Strict temperature control
Enzyme extraction	Asian bullfrog skin [67]	1–3% pepsin	22.6–28.3	High extraction efficiency, environmental friendly	Strict process requirements
	Porcine tissues [68]	1% pepsin	41–47		
Other extraction	Channel catfish skin [69]	Homogenization 7000 rpm, 5 min; pepsin 23.6 KU/g, pH 2.4	64.19	High extraction rate, fast process	Complex steps
	Cartilage of Siberian sturgeon [70]	0.5 M acetic acid, 1% porcine pepsin, 4 °C, 72 h	41.82		
	Chicken sternal cartilage [71]	Sonication 950W, frequency 20–25 kHz	85		
	Bovine tendon [72]	Ultrasonic irradiation 120 W, 40 kHz, 0.5 M acetic acid, pepsin	88		

commonly employed as a pretreatment and combination method with other extraction methods. Jaziri et al. [61] successfully extracted collagen from lizard fish skin by soaking the skin in 0.1 M NaOH solution with continuous stirring for 6 h to remove non-collagenous proteins and pigments, and then followed with an acid method. Nagai et al. [62] obtained the collagen by extracting small pieces of leafy Tibetan plum deer tendon in 0.1 M NaOH and then precipitate the collagen in 0.05 M Tris–HCl (pH 7.5) containing 2.2 M NaCl (Table 1).

2.3 Acid extraction

The acid extraction method mainly uses low-concentration collagen, because ions in medium will interfere with its intermolecular ionic bonds, causing the breakage of ionic and Schiff bonds. Five types of acids commonly used are acetic acid, hydrochloric acid, oxalic acid, citric acid and lactic acid [73]. For example, Abbas et al. extracted collagen from catfish skin, fins, head, bones and muscles using acetic acid [74]. Sylvia et al. [67] extracted collagen from Asian bullfrog skin using acetic acid and studied the effect of acid concentration on the yields and properties of the obtained collagen. They found that the optimum collagen yield and properties (e.g., thermal transition stability and α -amino acid content) were obtained at an acetic acid concentration of 0.75 M and a skin/acid solution ratio of 1:15 (w/v). Besides, Jaziri

et al. extracted collagen from lizard fish skin using acetic acid, lactic acid, and citric acid [48]. The results showed that all extracted collagen was classified as type I collagen with the presence of α chains ($\alpha 1$ and $\alpha 2$). The yield of collagen extracted using acetic acid (1.8 mg/g) was higher than that of lactic acid (1.6 mg/g) and citric acid (1.3 mg/g). To avoid the destruction of collagen peptide, the acid extraction method requires strict control of concentration, hydrolysis temperature and time. Moreover, it requires acid-resistant equipment, leading to the high cost of production (Table 1).

2.4 Hot water extraction

The hot water extraction process can hydrolyze collagen into peptides by disrupting the hydrophobic and hydrogen bonding between the amino acids of collagen via heating. Wu et al. [75] evaluated the hydrothermal stability of cross-linked collagen using a microthermal bench method under glycerol-water conditions. This method has strict temperature requirements, and the collagen loses its bioactivity once the extraction temperature is high. The degree of protein hydrolysis, the yield of collagen peptides, and the amount of free amino acids increased as the temperature rose to 150–190 °C. In contrast, the protein was severely hydrolyzed into small molecular peptides and amino acids at 190–240 °C [76]. To optimize the hot water extraction, Park et al. [66]

studied the critical roles of temperature (150–250 °C) and self-generated pressure (350–3900 kPa) of the hydrothermal hydrolytic process of collagen. The results showed that the extraction of collagen peptides using hydrothermal method at 190 °C (1100 kPa) was 56.9%. This method for the extraction of collagen peptides is environmentally friendly and effective, with the significant advantages of being non-toxic and safe (Table 1).

2.5 Enzyme extraction

Enzymatic extraction is a method to obtain enzymatically soluble collagen by cleaving the covalent bonds between lysine or hydroxylysine on the terminal peptide chains of collagen in acid conditions. Without affecting the triple helix structure, it degrades the peptide bonds in the non-helical region of collagen and generates unfolded peptide chains [77]. This method can maintain the excellent physical and biochemical properties of collagen. In general, the frequently used proteases are divided into three main categories: animal proteases, plant proteases and microbial proteases. The commonly used enzymes for enzymatic hydrolysis of collagen are pepsin, pancreatic protease, papain, ficin. Many factors have been reported to affect the enzyme extraction, such as temperature, pH value, reaction time, enzyme concentration, and the ratio of enzyme to substrate concentration. Lee [78], Mathew

[79] and Chen [50] used pepsin to extract collagen from human perinephric adipose tissue, hyaline nasal cartilage of Fortuna and scales of grass carp, respectively. In contrast, Felim et al. [80] extracted collagen from jellyfish using papain.

2.6 Other extraction methods

In order to obtain collagen with a high extraction rate, fast extraction speed and good structural integrity, several complex extraction methods have been developed. The common ones include enzyme and enzyme complex method, acid and enzyme complex method, ultrasonic-assisted method. Shaik et al. [81] sonicated the stingray skin samples by an ultrasound (20 kHz and 500 W) for 0.5 h. The resultant extracts were further purified by centrifugation (6500g for 15 min) at 4 °C, and the supernatant was re-extracted by 0.5 M acetic acid, resulting in a collagen extraction yield of $42.34 \pm 0.62\%$. Another classic example is the complex extraction method for bovine achilles tendon. To obtain alkaline insoluble collagen, pepsin and acetic acid were added for enzymatic digestion and the treated solution showed high viscosity. The collagen was then purified by salinization and dialysis. Collagen containing approximately 30% β -chain was obtained [82]. Tan et al. [69] extracted collagen from catfish skin with the aid of homogenization and the final

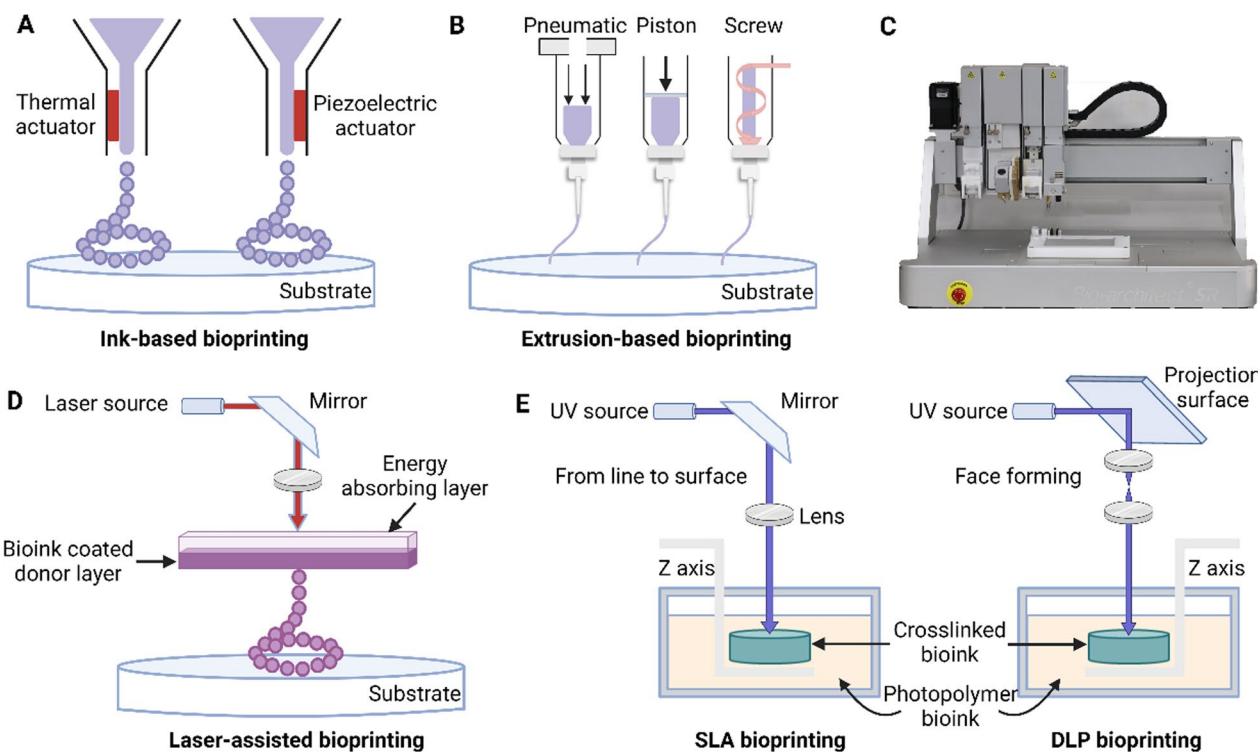


Fig. 3 The schematics of 3D printing technologies. **A** Inkjet-based bioprinting. **B** Extrusion-based bioprinting. **C** The image of a typical extrusion-based bioprinter. **D** Laser-assisted bioprinting. **E** Stereo lithography appearance (SLA) and digital light processing (DLP) bioprinting

extraction rate was 64.19%. Luo et al. [70] obtained collagen from Siberian sturgeon gristle using the combination of acetic acid and pepsin. The results revealed that the extraction rate of acid-soluble collagen was 27.13%, and the extraction rate of the combination method with enzyme was 41.82%.

3 3D printing methods for collagen-based biomaterials

Bioprinting technologies can be largely classified into three categories according to their fundamental printing principles (Fig. 3) [83], including inkjet-based bioprinting [84], pressure-assisted bioprinting [85], and light-assisted bioprinting [86]. Bioinks based on collagen have shown good printability using a range of different 3D printing techniques and they can be formulated as low viscosity fluids that can be extruded through a small nozzle [87]. This allows for the precise control of the placement and shape of the printed material in inkjet-based bioprinting. In light-assisted printing, the bioink, which can be utilized to produce high-resolution structures, is solidified selectively using a laser beam. This method allows for precise control of the printed material and can be used to create structures with high mechanical strength. However, it is worth noting that the printability of collagen-based bioinks depends on the formulation of the bioink, including its viscosity, gelation time and temperature, as well as the characteristics of the particular printing technique being employed [88].

The 3D printed cell-free scaffold can control both its internal pores and external shape to attract endogenous stem cells by creating a microenvironment favorable for cell growth and releasing bioactive molecules; or by inoculating cells directly onto the scaffold, which provides an ideal 3D space for cell adhesion, proliferation, and differentiation [88]. Since there are no living cells inside the scaffold, the scaffold material may be more carefully chosen and altered for improved function. In order to print biomimetic structures resembling organic and inorganic components of natural bone tissue, Kajave et al. [89] combined bioactive glass and methacrylated collagen and then demonstrated their effects on the preservation of human mesenchymal stem cell viability and the enhancement of alkaline phosphatase activity. Cell-laden bioprinting is the process of wrapping live cells in appropriate biomaterials to form a bio-ink to build the three-dimensional structure of the desired tissue or organ and the distribution of cells inside it in a 3D printed manner that can directly feed the cells to the specified site in the body. Muthusamy et al. [90] printed a three-dimensional stable structure of endothelial cells sandwiched between fibroblast layers after adding xanthan gum to type I collagen as a bioink for encapsulating cells. They

experimentally demonstrated that an interconnected capillary-like network could be formed in this structure, and the ability of this scaffold to produce blood vessels has potential applications in 3D bioprinting of various tissues and organs.

3.1 Inkjet-based bioprinting

Inkjet-based bioprinting is a type of 3D printing technique derived from the conventional desktop inkjet printing. It is a non-contact approach for producing 3D printed objects by depositing ink droplets on successive layers for biomanufacturing. The drop-on-demand inkjet printing can be classified according to the mechanism of how the droplets are ejected. For example, the thermal approach demonstrates a mechanism by which the liquid that is transformed into vapor after being released from the chamber through the print hole. Alternatively, the acoustic method utilizes a mechanical impulse to alter the shape of the piezoelectric crystal behind the print head to produce droplets for inkjet printing [91] (Fig. 3A).

To create well-structured 3D printed structures, inkjet printing enables the deposition of small-volume droplets containing cells or proteins at specific spatial locations [92]. Notably, it enables the highly precise location of cells and biological components in the both two-dimensional (2D) and 3D architecture for tissue engineering and many other applications [93] (Table 2). The technique also offers the benefits of high throughput and digital control. However, it suffers from the inherent limitation of the printing head to provide a continuous flow [90]. Additionally, printing cells in high densities is restricted by cell settlement or agglomeration due to the small orifice of the nozzles, which may also result in clogged print nozzles [94]. For instance, printing high-viscosity hydrogels, such as those commonly used for cartilage tissue engineering, can be challenging due to the limitations in droplet formation and printhead clogging. As a result, only lower concentrations of droplets can be printed, and bioinks must exhibit low viscosity (< 10 mPa s) and cell density ($< 10^6$ cells/mL) [95], which results in the poor mechanical properties of the printed structures.

3.2 Extrusion-based bioprinting

Extrusion-based bioprinting can produce personalized scaffolds with a certain mechanical strength by utilizing pneumatic pressure or mechanical force to drive the bio-ink out of the nozzle using a piston or screw [96] (Fig. 3B, C). For example, cell-laden hydrogels or cell spheroids are deposited onto the substrate by pneumatic or motorized plungers to create a custom three-dimensional design [12]. The primary advantage of this method is its capacity to be scaled up due to the continuous flow of bioink and

Table 2 Pros and cons of different 3D printing techniques

Printing techniques	Resolution	Pros	Cons
Inkjet-based bioprinting	About 100 μm	Low cost; high print speed; High cell survival rate (80–90%)	Low cell viscosity and density; Easily clogged nozzles; Unreliable cell encapsulation
Extrusion-based bioprinting	> 100 μm	Ability to print high cell densities models	Limited resolution; Low print speed; Low probability cell viability
Light-assisted bioprinting	10–50 μm	High resolution, good cell viability (> 95%)	High cost, less efficient

the high deposition rates [97] (Table 2). Moreover, the high viscosity and high cell concentration of the bioink is comparable to natural tissues. It is notable that the shear stress, which is dependent on the nozzle diameter, might affect cell viability [98]. Therefore, one of the key issues is to maintain cell viability and print speed while reducing pressure or nozzle size.

Montalbano et al. [99] developed a multiphase bio-material ink suitable for extrusion printing, which combines type I collagen with nano-hydroxyapatite and mesoporous bioactive glass particles. When the multiphase system at 10 °C was subjected to increasing shear rate, the viscosity values decreasing from approximately 206.7–0.17 Pa s. This is particularly advantageous for materials intended for 3D printing, as it allows for proper extrusion. Lee et al. [100] designed a novel extrusion-based bioprinting method that can be used to prepare microfluidic channels of collagen-based biomaterials for organ-on-a-chip. Collagen hydrogels with a thickness of 400 μm were printed in pre-designed fluidic channels (1.5 mm \times 1.5 mm \times 15 mm) for diverse organ-on-a-chip systems and liver microarrays. The bioprinting with cell-laden hydrogel bioink successfully positioned different cell types and collagen-based biologic materials at the desired locations, eliminating the process of cell inoculation. It also exhibited improved printing accuracy and reduced protein absorption. The method is easy and versatile for organ-on-a-chip production, which makes it possible to mimic an organ completely such as oral tissues.

3.3 Light-assisted bioprinting

Odde et al. [101] first introduced a laser-guided direct writing for 2D cell patterning processing. This laser-assisted printing is able to print moderately viscous biological materials while avoiding direct contact between the printhead and the bio-ink, which causes negligible mechanical stress to the cells and maintains high cell viability [102] (usually higher than 95% [103]). More common light-assisted bioprinting involves several techniques including laser-induced forward transfer (LIFT), stereo lithography appearance (SLA), and digital light processing (DLP).

LIFT can take place from liquid or solid phases [104]. In a typical scenario, a drop of bioink is moved from bioink-coated donor layer onto a receiver, when a laser is absorbed by a laser energy absorbing layer (e.g., a thin layer of gold) (Fig. 3D) [105]. The high lateral resolution is only defined by the laser spot size. For example, after the laser is emitted by the laser pulse generator, the laser energy absorbing layer harvests the laser and generates localized heating [106]. The bioink attached to the downward side of the absorbing layer is then evaporated by the heat to form a high-pressure bubble, which is eventually deposited on the receiving substrate, forming the programmed pattern. In contrast, SLA and DLP are relatively new printing methods (Fig. 3E). SLA employs point or line scan of laser to induce the polymerization of photopolymers, which form a complex 3D construct from a photopolymer bath. Different from the SLA, the laser of DLP bioprinting is modulated by a digital micromirror device (DMD). DMD contains several hundred thousand microscopic mirrors arranged in array and can project images onto the photopolymer bath, which is more efficient than SLA. Overall, all of them fabricate scaffolds with high structural fidelity, good cell viability and intricate geometric characteristics (Table 2). Wu et al. [107] developed a novel collagen-based bioink suitable for DLP 3D bioprinting. Collagen methacrylate was first synthesized and the degree of substitution was successfully increased by raising the pH value during the synthesis. Then, lithium phenyl(2,4,6-trimethylbenzoyl) phosphinate and procyanidins (PA) were introduced into the bioink as UV photoinitiators and crosslinkers to provide fast light-curing capability, which turns into a stable hydrogel after 30 s of UV irradiation. For example, the hydrogel containing 40 $\mu\text{g}/\text{mL}$ PA had the highest final storage modulus (14,862 Pa) after 150 s of UV irradiation at 10 mW cm^{-2} , which was 10 times higher than that of the hydrogel without PA.

4 Application of 3D bioprinting collagen in oral medicine

4.1 Pulpal nerve and vascular regeneration

Conventional root canal treatment weakens the affected tooth by removing the nerves and blood vessels from the pulp, causing loss of sensation and a lack of nutrient

supply to the tooth. In such context, the restoration of dentin and the recovery of nutrition supplied to nerves and blood vessels are the essential factors for pulp regeneration [108].

Collagen is a common substance for nerve regeneration [109, 110]. Lee et al. [111] developed a straightforward cell printing method to form neural cell patterns in multilayered collagen hydrogel. In this design, collagen layers were first printed to provide a scaffold for the cells. Then, rat embryonic neurons and astrocytes were deposited on top of the existing layers. 3D cellular

hydrogel complexes were synthesized by repeating this process. This work testified the capacity of microvalve printing to build various cellular patterns in a single unit. Moreover, the partially hydrolyzed products of collagen (i.e., gelatin) can gel in the presence of 1-ethyl-3-(3-dimethylaminopropyl) carbodiimide (EDC)/N-hydroxysuccinimide (NHS). The cross-linked gel shows improved physical, chemical and handling properties [112]. In this case, living cells from various tissues were added to bioprinted composite gelatin hydrogels to promote the fabrication of cell-laden functional materials

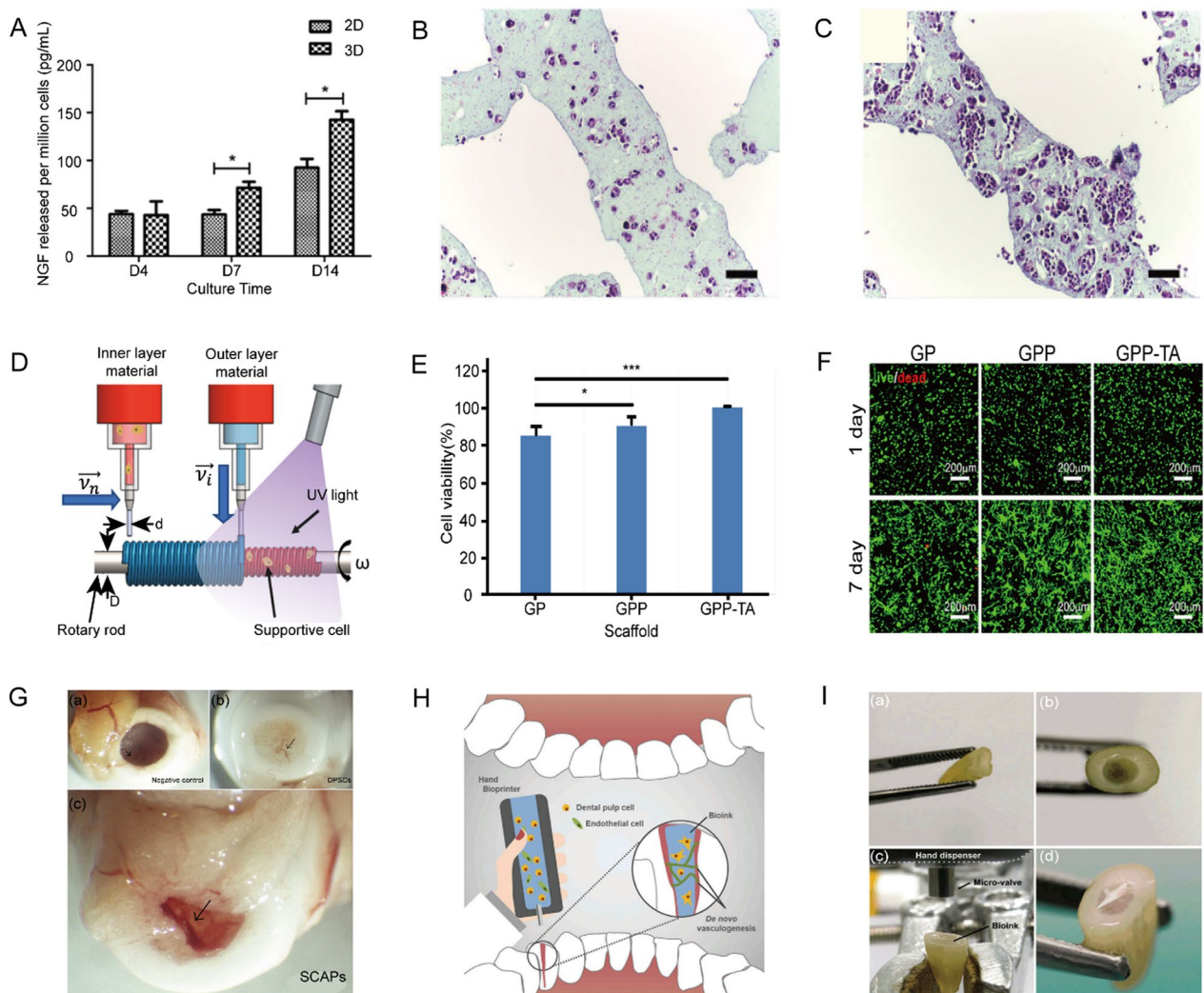


Fig. 4 **A** Nerve growth factor released from 3 and 2D cultured cells on Day 4, 7 and 14. **B** and **C** Cell-laden constructs on Day 7 and Day 14. Reprinted with permission from Reference [113]. **D** Schematic diagram of the additive-lathe 3D bioprinting device for the fabrication of two-layer nerve conduits. Reprinted with permission from Reference [114]. **E** Cell viability of NSCs in different materials. “*” means the significant difference between different groups (* $p < 0.05$, ** $p < 0.01$, *** $p < 0.001$). **F** Confocal fluorescent images of stained NSCs embedded in different materials on Day 1 and 7. Reprinted with permission from Reference [115]. **G** Macroscopic assessment of blood vessel ingrowth after 12 weeks of transplantation. Reprinted with permission from Reference [116]. **H** Schematic diagram of pulp regeneration by in-situ bioprinting with a hand-held printer. **I** Photos of human tooth roots before and after 3D print. Reprinted with permission from Reference [117]

for biomimetic artificial structures. Li et al. [113] built a 3D microenvironment for rat Schwann cell (SC) *in vitro* using a customized alginate–gelatin hydrogel. The results showed that rat Schwann cells in the bioprinted scaffolds showed higher viability and more proliferative than the cells in 2D culture dishes. Meanwhile, the amount of nerve growth factor released by rat Schwann cell RSC96s in the scaffold was also higher than that of the cells in culture dishes after 2 weeks of cultivation (Fig. 4A). HE stained images further showed the growth of RSC96 cells in the printed alginate-gelatin hydrogels during the experiment (Fig. 4B, C).

The performance of 3D printed structures varies with the design and composition. For example, printed nerve conduits should exhibit distinct properties in terms of permeability, flexibility, degradability, and nerve regeneration. Dixon [118] and Yu et al. [119] reviewed the existing design for conduit, including material selection, cell and protein inclusion, and their mechanical properties. Ideally, supporting cells (e.g., SCs, macrophages, and replacement cells), supplementary biomolecules (e.g., neurotrophic factors and matrix proteins) and architectures (e.g., tubular lumen) can be strategically integrated to mimic the arrangement of a nerve, which provides physical and biological properties. It is notable that peripheral nerves are not fully reinnervated when the injury gap is wide. To overcome these challenges, Liu et al. [114] developed a multi-nozzle additive-lathe bioprinting technique to manufacture a two-layer nerve conduit (Fig. 4D). The nerve conduit consists of an outer layer based on GelMA/poly (ethylene glycol) diacrylate (PEGDA) and an inner layer based on gelatin methacrylate (GelMA). The porosity and average pore size of the outer layer were $29.78 \pm 3.94\%$ and $14.94 \pm 2.84 \mu\text{m}$, while those of the inner layer were $53.31 \pm 11.51\%$ and $41.27 \pm 8.08 \mu\text{m}$. This hierarchical structure enabled a high water content of the inner layer and better cell viability. In addition, the interior and exterior layers were smoothly connected, which is crucial for improving the mechanical strength of the nerve conduit.

The poor electrical conductivity of the current 3D bioprinted scaffolds impedes the bioelectrical signal transmission between cells, restricting the therapeutic efficacy for nerve tissue repair [119, 120]. To this end, Song et al. [115] developed a 3D bioprinted electroconductive hydrogel scaffold (GPP) composed of neural stem cell (NSC), GelMA, PEGDA, and poly(3,4-ethylene dioxythiophene) (PEDOT). The scaffold has moderate mechanical strength and good electrical conductivity, which substantially enhances the exchange of bioelectrical signals among neurons. Compared with pristine GelMA/PEGDA hydrogel (GP), PEDOT was introduced as conductive polymers. Additionally, the

GPP scaffold can be modified with tannic acid (TA), generating a new type of electroconductive hydrogel (i.e., GPP-TA). According to the results of the quantitative analysis, it was found that the proportion of neuron-specific Tuj-1 positive cells in the 3D GPP-TA scaffold was $49.3 \pm 7.8\%$, significantly higher than that of GPP scaffold ($24.1 \pm 5.6\%$) and GP scaffold ($37.1 \pm 4.1\%$). These results provide strong evidence that electron propagation in the scaffold can be facilitated by modulating the components of the 3D GPP-TA scaffold, thereby enhancing nerve regeneration. (Fig. 4E). The fluorescence images showed that all three hydrogels had a high survival rate in 1-day culture (Fig. 4F). For better biocompatibility of scaffolds to NSCs and oligodendrocytes (OLG), Liu et al. [121] developed a scaffold based on sodium alginate/gelatin printing that was incorporated with neural stem cells and oligodendrocytes. These cells were involved in myelin formation of neuronal cell axons. This scaffold enhances spinal cord repair after injury, and are effective vehicles for cell transplantation for spinal cord injury. Live/dead cell staining showed good viability of NSCs and OLGs in the scaffold. The average cell survival rate was about 83% after 3 days and dropped to 76% after 5 days. A large number of surviving NSCs and OLGs could be observed in the hydrogel. Notably, OLGs are particularly sensitive to the acute injury environment in the scenario of spinal cord injury. Apoptosis of OLGs begins hours after injury and lasts for several weeks, particularly detrimental to demyelination. These results demonstrated the superior biocompatibility of the 3D bioprinted sodium alginate/gelatin scaffold, indicating the great promise for regeneration of functional vascular and neural tissues.

In addition to the exploration of printed pulpal nerves, researchers have also expanded the application of bioprinting to blood vessels. Adequate vascular supply is essential for tissue survival in the field of dental regeneration [122]. It is usually improved by adding stem cells or appropriate angiogenic growth factors. Preliminary results showed that the cell survival rate of dental pulp stem cells (DPSCs) embedded in 3D printed alginate-gelatin hydrogels can achieve 87% [123]. Duarte Campos et al. [124] put forward a novel *ex vivo* strategy to apply cell-loaded bioinks on dental defects by means of a handheld drop-on-demand bioprinter. The bioinks consisted of agarose and collagen type I, and the seed cells included dental pulp cells (hDPCs) and human primary umbilical vein endothelial cells (HUVECs). Vascularization was observed both in cell-loaded bioinks cultivating in 3D discs and in the case of bovine teeth after 2 weeks, which demonstrated that this *in situ* bioprinting expanded the toolbox for the treatment of root canal-forming vessels in teeth. Hilken et al. [116] constructed a complex dentin/pulp-like tissue with a vascular system by 3D printing

using DPSC to compare their regenerative potential and confirm their previously established paracrine angiogenic properties. Angiogenic properties of in-scaffold DPSC were assessed by enzyme-linked immunosorbent assay against vascular endothelial growth factor (VEGF). After 14 days of culture, the medium of the constructs contained high amounts of VEGF, which further increased after 28 days of culture. The tissue color and the apparent vascularity differed between the experimental groups. (Fig. 4G). Although the constructs containing DPSC and/or SCAP did not show higher rates of vascularization compared to control constructs, these results proved that 3D printing of capillaries is feasible. Duarte Campos et al. [117] used a hand-held bioprinter to print cell-loaded bioink directly onto human isolated teeth (Fig. 4H). The bioink consisted of agarose and type I collagen, and the seeded cells included dental pulp cells and human umbilical vein endothelial cells. Both of the seeded cells were observed to form blood vessels after culture (Fig. 4I), indicating that handheld bioprinting may encourage in situ blood vessel formation and thus pulp regeneration. To our knowledge, the use of 3D bioprinting for pulp regeneration are still lacking in the literature.

4.2 Cartilage regeneration

Cartilage tissues in the craniofacial region mainly include temporomandibular joint (TMJ) discs, auricular cartilage, and nasal cartilage. The main chemical components of cartilage are water, collagen and proteoglycan [125]. Highly organized cartilage with fine structure fulfills specific functions such as bearing mechanical loads, distributing pressure and reducing friction [91]. Bioinks for cartilage reconstruction should be able to mimic three-dimensional structures with mechanically anisotropic, nonlinear, and viscoelastic behavior of native cartilage [126].

One of the first studies using pure collagen bioinks for cartilage bioprinting was conducted in 2016 [127]. This research was designed to establish a method for 3D bioprinting with high-density collagen hydrogels and investigate the properties of the printed constructs (e.g., cell viability, structural fidelity, mechanical strength) (Fig. 5A). These constructs are mechanically stable and capable of supporting cell growth. The data showed that heated substrate greatly improved the geometric precision of the printed products. For example, when using 17.5 mg/mL collagen, the structural fidelity of the products increased from 66 to 79% upon heating condition. Regarding stiffness, a gradient from 12.5 to 17.5 mg/mL led to the change of 130% in stiffness. This study implies the advantages of the thermal deposition of printable collagen formulations in improving geometric accuracy.

Yang et al. [128] appraised three different combinations including alginate (SA), alginate/agarose (SA/AG), and alginate/collagen (SA/COL) for 3D bioprinting. The results suggested that the scaffolds of SA/AG and SA/COL bioinks exhibited higher compressive modulus and tensile strength compared to SA alone. Compared to SA, the compressive modulus increased by nearly 2.38 times and 1.87 times, and their tensile strength increased by 124.5% and 162.1%, respectively. In addition, the SA/AG constructs presented more cell adhesion to the scaffold compared to SA alone printing. However, the cell survival rate was higher for SA/COL bioconfluent compared to SA/AG and SA. The chondrocyte phenotype was well maintained when cells were imprinted onto the SA/COL.

3D printing is able to mimic the extracellular matrix nanofiber structures and biological environment. According to a report by Nguyen et al. [132], multilayered collagen/ γ -polyglutamic acid/hydroxyapatite (Col/ γ -PGA/HA) composite scaffolds were synthesized by 3D printing technology. HA/ γ -PGA formed the bottom layer and Col/ γ -PGA formed the layers from second to fourth. Rat bone marrow mesenchymal stem cells (rBMSCs) and human adipose-derived stem cells (hADSCs) were cultivated on the 3D constructs and their activities were also evaluated including cell adhesion, proliferation, and differentiation. Moreover, animal experiments (e.g., rat and nude mice models) were further conducted. The obtained scaffold exhibited good mechanical properties and biocompatibility, and facilitated the upregulation of osteochondrogenesis in both cell and animal experiments, which demonstrated its potential of osteochondral regeneration. Fahimipour et al. [129] developed another platform for osteogenic differentiation of hDPCs based on the systematic properties of hybrid scaffolds (Fig. 5B). In contrast to 3D printed beta-tricalcium phosphate (β -TCP) scaffolds, the hybrid scaffolds made from β -TCP/collagen provided improved proliferation and alkaline phosphatase (ALP) activity of hDPCs. In addition, the binding of TCP to the collagen matrix was found to enhance ALP activity (Fig. 5C, D). After 3 weeks, DPCs were more proliferative on β -TCP/Col-TCP than on the β -TCP/Col (Fig. 5E, F). Figure 5G showed an increased cell attachment and proliferation on 3D printed β -TCP scaffold.

3D printing has also been employed to engineer scaffolds and regenerate multi-tissue interfaces for temporomandibular joint repair. Helgeland et al. [130] fabricated a scaffold printed with porcine gelatin type A and the printed structures were then cross-linked using a 1% (w/v) dynein solution at room temperature for 48 h. The cross-linked samples showed a compressive Young's modulus of 4.52 ± 1.51 MPa, after immersion in PBS the Young's modulus of the cross-linked

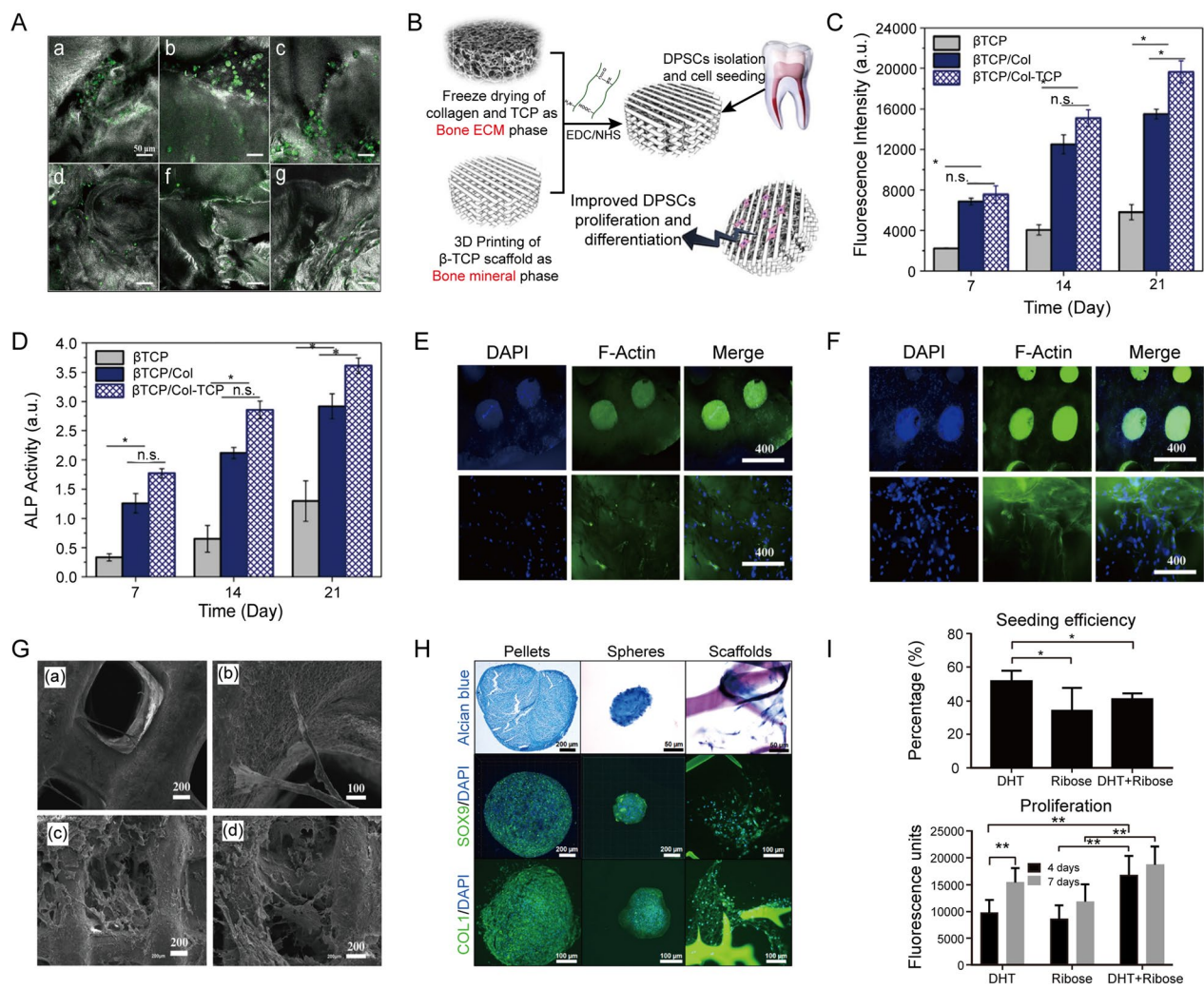


Fig. 5 **A** Confocal reflectance images of the fibrocartilage cell loaded scaffolds at different concentrations (12.5, 15.0 and 17.5 mg/mL) of collagen. Reprinted with permission from Reference [127]. **B** Collagenous matrix supported by a 3D-printed scaffold for osteogenic differentiation of dental pulp cells. **C** Comparison of the viability of DPSCs on different 3D-printed scaffolds (β -TCP, β -TCP/Col and β -TCP/Col-TCP scaffolds) during 3 weeks. **D** ALP activity of DPSCs cultured on different 3D-printed β -TCP scaffolds after 1, 2, and 3 weeks. **E** The growth of DPSCs on β -TCP/Col and **F** β -TCP/Col-TCP scaffolds after 3 weeks of culture. **G** SEM images of DPSCs on 3D printed β -TCP scaffolds and β -TCP/Col-TCP scaffolds after 3 weeks. Reprinted with permission from Reference [129]. **H** After 21 days, Alcian blue and immunofluorescence staining. Green (SOX9 and COL1). Blue (DAPI). Alcian blue staining shows the glycosaminoglycan (GAG) content on the scaffold filaments. Reprinted with permission from Reference [130]. **I** Cell seeding efficiency and proliferation of rBMSC on printed scaffolds ($n=8$). $*p \leq 0.05$; $**p \leq 0.01$. Reprinted with permission from Reference [131]

samples decreased significantly to 191 ± 0.01 kPa. Scaffolds on human bone marrow-derived mesenchymal stem cells (hBMSC) for chondrogenic differentiation were compared to cell precipitation and spheroids with a cell inoculation efficiency of $3.7 \pm 3.4\%$ after 57 h. All groups exhibited increased expression of all genes from day 4 to day 21. Pellets, spheroids and scaffold sections were stained for Alcian blue after 9 days (Fig. 5H). The results indicate that 3D printed gelatin-dye wood scaffolds supported the viability, attachment

and cartilage differentiation of hBMSCs. To improve the physical properties of 3D printed gelatin scaffolds for cartilage regeneration, Helgeland et al. [131] further explored the structure and properties of scaffolds after dual cross-linking by dehydrogenation heat (DHT) and ribose glycation, to study the response of rat bone marrow-derived mesenchymal stem cells (rBMSC) inoculated onto experimental scaffolds. Cell attachment, viability, proliferation, and chondrogenic differentiation were evaluated in this process. The results showed that the seeding efficiency of the dual cross-linked scaffolds

was lower than that of the DHT group by 40%. At Day 4 and 7, dual-crosslinked scaffolds had higher DNA amounts compared to other groups. The cell proliferation on it was also higher (Fig. 5 I). The degree of crosslinking was $14.5\% \pm 1.9\%$ for DHT, $31.8 \pm 5.6\%$ for ribose and $44.4 \pm 8.5\%$ for double cross-linked samples. The double crosslinked motifs demonstrated the highest gene expression level after 21 days. Research shows that the manufactured scaffold allows for the growth of bone and cartilage, particularly forming a dynamic mineralized interface tissue between the cartilage and subchondral bone. These studies validate the implementation of 3D bioprinting technique in cartilage regeneration.

4.3 Periodontal tissue regeneration

Periodontal diseases are one of the most common infectious diseases worldwide, which cause the damage of periodontal support tissues, tooth loss, and even mastication dysfunction, thereby significantly affecting quality of life for patients [133]. The aim of periodontal treatment is to control the infection and re-establish periodontal tissue lost. Regeneration periodontal surgery is one of the first tissue engineering methods applied in the medical profession [134]. Challenges still remain in regenerating the periodontal complex, including the alveolar bone, periodontal ligament (PDL), and cementum [5]. The PDL is a soft, dense connective tissue consisting of dense collagen fibers (type I and type III) arranged in organized orientations [135]. The fibers of the periodontal ligament are arranged perpendicular to the dental bed and the alveolar bone, which connect the cementum to the alveolar bone [136]. For example, the ends of the ligament (i.e., Sharpey fibers) which are attached to the cementum play essential roles in stabilizing the tooth roots, transmitting occlusal forces and proprioceptive information, and ensuring nerve sensitivity [137]. Traditional periodontal treatments have been established to rebuild these dental structures by surgical or non-surgical strategy, but the initial function of the periodontal tissues remains poor [138]. Recently, 3D bioprinting techniques have been applied to the field of periodontal regeneration to develop layered scaffolds that can mimic the properties and structural configuration of the periodontium, which consists of soft tissue (e.g., gingiva, periodontal ligament) and hard tissue (e.g., bone, cementum).

The fabrication of biomaterials that can mimic an appropriate biological microenvironment remains difficult in periodontal treatment [139]. Elango et al. [139] presented the use of a 3D biomaterial matrix fabricated with collagen, sodium alginate and titanium oxide (TiO_2) to generate an *in vivo* microenvironment, which allowed human periodontal ligament fibroblasts (HPLF) for

osteogenesis. The effect of 3D substrates on osteogenic differentiation enhanced osteocalcin secretion levels in HPLF cells compared to 2D cell cultures. The stiffness, shrinkage coefficient, water binding capacity, swelling rate and porosity of the collagen-based 3D (CB3D) matrix were determined to be 10.32 ± 1.78 MPa, $69.80 \pm 3.65\%$, $534 \pm 27.6\%$, $159.06 \pm 10.35\%$ and $87.61 \pm 8.21\%$, respectively, which are applicable in periodontal applications. After staining the minerals accumulated by differentiated HPLF cells using alizarin red stain, positive controls and cells cultured in this matrix showed high intensity mineral staining, indicating that HPLF cells cultured in this collagen-based matrix have the ability of osteogenic differentiation (Fig. 6A). In contrast to the control and positive control groups, differentiated HPLF cells also exhibited increased quantities of collagen, osteocalcin, and Runx2 protein ($p < 0.05$) (Fig. 6B, C). The stiffness and porosity of these manufactured 3D structures modulated the desirable biological microenvironment and molecular interface for promoting periodontal tissue regeneration.

The ideal restoration of PDL microarchitecture benefits from the use of biomimetic scaffolds that direct PDL development. Lin et al. [142] developed a biomimetic collagen-based waveform microfibrils by an extrusion-based bioprinter, which promoted the growth of PDL cells. A bioreactor based on laminar flow was employed to mimic the shear stress in the fluids. PDL cells were inoculated onto their corresponding microfibrils for 1–4 h in the presence of suitable fluidic shear stress (0 or 6 dynes/cm²), while their viability, morphology, growth patterns and the level of gene expression were monitored. The results revealed that the 3D printed collagen-based waveform microfibrils were able to withstand shear loading. Particularly, the viability of PDL cells was maintained and they showed the potential to facilitate the enhanced tissue regeneration. To achieve complete tissue regeneration, materials with multifunctional and layered structures are important. Lee et al. [20] designed a heterogeneous scaffold with a delicate structure and biochemical gradient. This scaffold consists of three different components in correspondence with the morphological characteristics of periodontal complexity, including cementum, periodontal ligament and alveolar bone. Each layer had a distinct structure with different apertures (i.e., 100 , 600 and 300 μm). The cementum, periodontium and bone areas were arranged in a hierarchical structure. These parameters were selected based on physiological microbiological characteristics, which were in accordance with recent soft and hard tissue regeneration studies [143, 144]. Liu et al. [140] fabricated a silk fibroin/collagen/hydroxyapatite (SCH) scaffold by cryogenic 3D printing and loaded it with recombinant human erythropoietin (rh-EPO) for the reconstruction of alveolar bone defects (Fig. 6D).

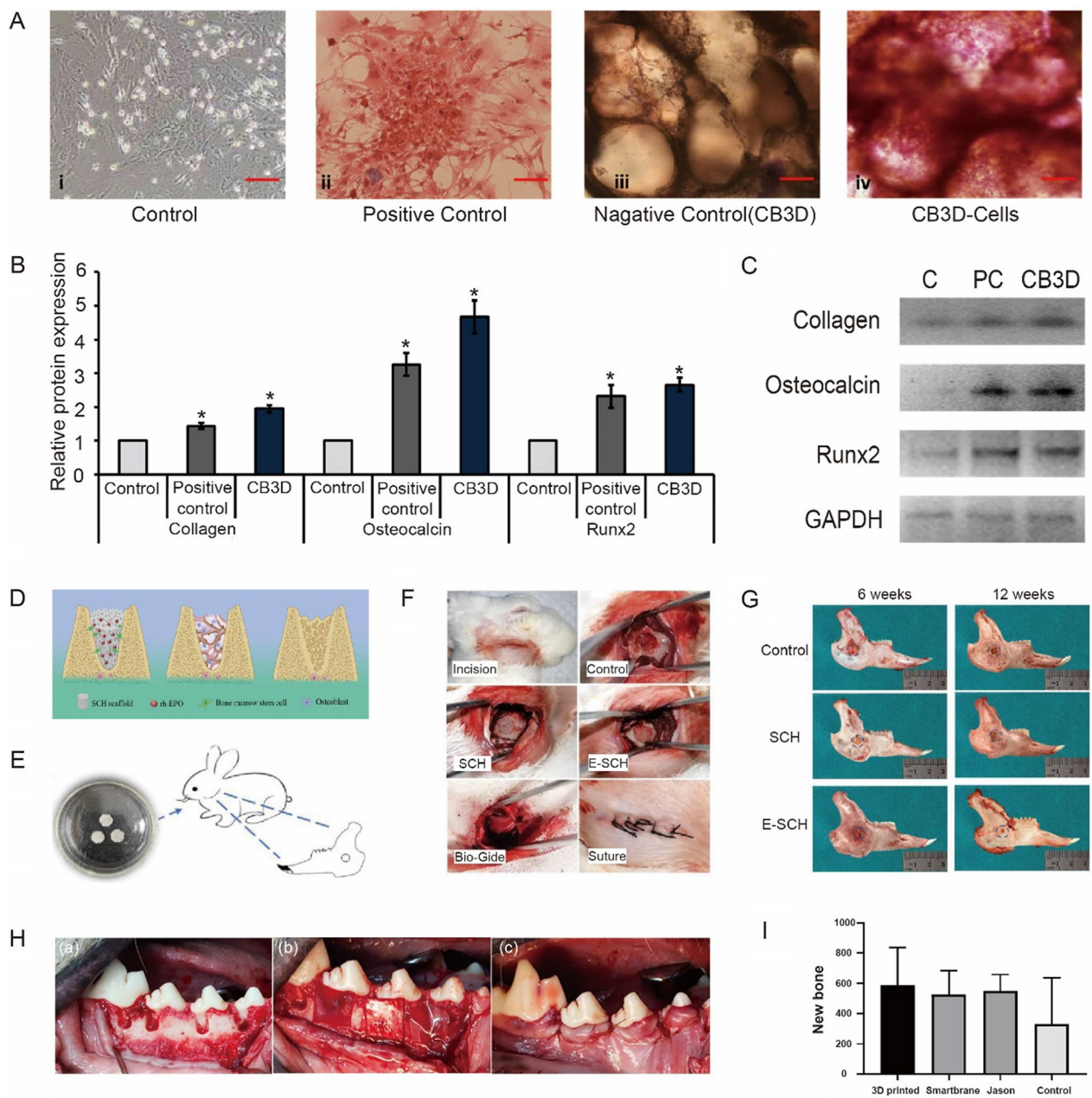


Fig. 6 **A** Alizarin red staining for mineral distribution of differentiated HPLF cells. (i) Cells cultured in fibroblast medium (control, C), (ii) cells cultured in osteogenic induction medium (positive control, PC), (iii) no cells in 3D matrix (negative control), and (iv) cells differentiated in 3D matrix (CB3D cells). **B** and **C** Protein expression (i.e., collagen, osteocalcin, and Runx2) in HPLF cells with or without 3D matrix. Runx2: Runt-related transcription factor 2, * $p < 0.05$ ($n = 3$). Reprinted with permission from Reference [139]. **D** Schematic diagram of repairing alveolar bone defect with E-SCH scaffold; SCH: silk fibroin/collagen/hydroxyapatite; rh-EPO: recombinant human erythropoietin. **E** Schematic diagram of mandibular reconstruction. **F** The preparation process of a rabbit mandibular defect model. **G** Rabbit mandible at 6 and 12 weeks after surgery. Reprinted with permission from Reference [140]. **H** Surgical procedure for the preparation of surgically induced dehiscence defects on maxillary premolar teeth using different membranes for restoration. From left to right: formed defects; placement of the membranes; flap and suturing. **I** Comparison of the four study groups using different membranes for maximum new bone thickness (μm). Reprinted with permission from Reference [141]

Also, they verified the bone repair ability of the scaffold by co-culture with cells and implantation in a rabbit mandibular bone defect model (Fig. 6E). It was found

that the SCH scaffold loaded with rh-EPO (E-SCH) better promoted the repair and regeneration of mandibular defects (Fig. 6F, G). The examination of the bone volume

fraction (BV/TV) at 12 weeks of implantation showed that the E-SCH group ($46.695 \pm 5.620\%$) was considerably greater than the control group ($39.063 \pm 2.413\%$) compared to the SCH group ($24.040 \pm 4.126\%$). Another study [141] showed the group treated with 3D printed membranes had improved new bone formation (Fig. 6H). Bone cement formation was also faster in the membrane groups compared to the control group, although there was no significant difference between the three membrane groups using Botiss Jason membrane (Botiss Biomaterials GmbH, Germany), Smartbrane membrane (Regedent, Switzerland) and 3D-printed membrane (Fig. 6 I). Periodontal regeneration using the three-phase scaffolds is relatively unexplored in clinical implementation, because the complicate spatial–temporal outcomes of periodontal regeneration. For example, the production and incorporation of the cement layer on the dentin surface of the root is the biggest challenge.

5 Conclusion remarks and perspectives

In conclusion, 3D printing is a versatile and precise fabrication technique that can create cost-effective and customized constructs with various biomaterials for oral medicine. We overviewed a variety of printable materials and recent advances in this field. Collagen-based bioinks can be used to print wound dressings that mimic the skin's natural extracellular matrix to promote rapid wound healing. 3D structures can also be printed to replicate the natural extracellular matrix of specific tissues, such as cartilage, bone and blood vessels. It is also possible to print 3D structures for use as drug delivery systems and adapt the composition of collagen-based bioinks to time-release drug delivery.

Although great progress has been made in recent years, the current 3D printed collagen scaffolds for oral medicine have some drawbacks. Collagen scaffolds used in 3D bioprinting for oral medicine often lack sufficient mechanical strength. This can result in the scaffolds being unable to withstand the forces exerted within the oral cavity, leading to deformation or failure. Current 3D bioprinting techniques struggle to reproduce the intricate structural complexity required for oral tissues, as the oral cavity consists of multiple specialized tissues, such as teeth, gums, and salivary glands, with unique architectures and functionalities. It often falls short in replicating these complex structures accurately. To optimize the biomaterials for 3D bioprinting in oral medicine, researchers can incorporate other biomaterials, such as bioceramics or synthetic polymers, into collagen scaffolds to enhance their mechanical strength. We envision that mimicking the original tissue (both internal structure and exterior shape) and emerging biomaterials with reliable properties and low costs will further push this technology to the

forefront of oral medicine. As a concluding remark, 3D bioprinting of collagen-based materials is a promising tool in oral medicine.

Abbreviations

GBD	Global burden of disease
3D	Three-dimensional
2D	Two-dimensional
Gly	Glycine
SLA	Stereo lithography appearance
DLP	Digital light processing
LIFT	Laser-induced forward transfer
DMD	Digital micromirror device
RTT	Rat tail tendon
EDC	1-Ethyl-3-(3-dimethylaminopropyl) carbodiimide
NHS	N-Hydroxysuccinimide
SC	Schwann cell
GelMA	Gelatin methacrylate
PEGDA	Poly(ethylene glycol) diacrylate
GP	GelMA/PEGDA hydrogel
GPP	3D bioprinted electroconductive hydrogel scaffold
NSC	Neural stem cell
PEDOT	Poly(3,4-ethylene dioxythiophene)
TA	Tannic acid
OLG	Oligodendrocytes
DPSCs	Dental pulp stem cells
hDPCs	Dental pulp cells
HUVECs	Human primary umbilical vein endothelial cells
SCAPs	Stem cells from the apical papilla
VEGF	Vascular endothelial growth factor
TMJ	Temporomandibular joint
SA	Alginate
AG	Agarose
COL	Collagen
PGA	Polyglutamate acid
HA	Hydroxyapatite
rBMSCs	Rat bone marrow mesenchymal stem cells
hADSCs	Human adipose-derived stem cells
β -TCP	Beta-tricalcium phosphate
ALP	Alkaline phosphatase
PDL	Periodontal ligament
HPLF	Human periodontal ligament fibroblasts
C	Control cells
PC	Positive control cells
CB3D	Collagen-based 3D matrix cultured cells
PA	Procyanidins

Acknowledgements

This work is supported by the Fundamental Research Funds for the Central Universities. This work is supported by grants from the National Natural Science Foundation of China (82100961) and Sichuan University postdoctoral interdisciplinary Innovation Fund.

Author contributions

JJZ, HL, YYH and WL made substantial contributions to the conception, design and revision of this review. BSY and HL wrote the manuscript. BSY downloaded and summarized related literatures. JJZ, BSY and HL designed and retouched all figures and tables. LLJ and YWZ participated in the corrections of figures and revision of this review. CLS and XX participated in the revision of this review. All authors read and approved the final manuscript.

Availability of data and materials

The datasets analyzed in this review are available as quoted and listed in the "References" section which have been specified in the article. We have obtained permission from the copyright holder to reproduce figures (or tables) that have previously been published elsewhere.

Declarations

Competing interests

Wei Lin is a member of the editorial board of *Collagen and Leather*. Jiajing Zhou and Yiyuan Han are members of the young editorial board of *Collagen and Leather*. They were not involved in the editorial review, or the decision to publish this article. All authors declare that there are no competing interests.

Author details

¹College of Biomass Science and Engineering, Key Laboratory of Leather Chemistry and Engineering of Ministry of Education, National Engineering Laboratory for Clean Technology of Leather Manufacture, Sichuan University, Chengdu 610065, China. ²State Key Laboratory of Oral Diseases, National Clinical Research Center for Oral Diseases, Department of Oral and Maxillofacial Surgery, West China Hospital of Stomatology, Sichuan University, Chengdu 610065, China. ³Laboratory for Biomaterials and Drug Delivery, Department of Anesthesiology, Division of Critical Care Medicine, Boston Children's Hospital, Harvard Medical School, Boston, MA 02115, USA.

Received: 15 May 2023 Revised: 7 July 2023 Accepted: 11 July 2023
Published online: 31 August 2023

References

- Peres MA, Macpherson L, Weyant RJ, Daly B, Venturelli R, Mathur MR, et al. Oral diseases: a global public health challenge. *Lancet*. 2019;394(10194):249–60.
- Chen X, Daliri EB, Kim N, Kim J, Yoo D, Oh D. Microbial etiology and prevention of dental caries: exploiting natural products to inhibit cariogenic biofilms. *Pathogens*. 2020;9(7):569.
- Pitts NB, Zero DT, Marsh PD, Ekstrand K, Weintraub JA, Ramos-Gomez F, et al. Dental caries. *Nat Rev Dis Primers*. 2017;3(1):1–16.
- Caton J, Nyman S, Zander H. Histometric evaluation of periodontal surgery. II. Connective tissue attachment levels after four regenerative procedures. *J Clin Periodontol*. 1980;7(3):224–31.
- Tonetti MS, Jepsen S, Jin L, Otomo Corgel J. Impact of the global burden of periodontal diseases on health, nutrition and wellbeing of mankind: a call for global action. *J Clin Periodontol*. 2017;44(5):456–62.
- Pihlstrom BL, Michalowicz BS, Johnson NW. Periodontal diseases. *Lancet*. 2005;366(9499):1809–20.
- Obregon F, Vaquette C, Ivanovski S, Huttmacher DW, Bertassoni LE. Three-dimensional bioprinting for regenerative dentistry and craniofacial tissue engineering. *J Dent Res*. 2015;94(9_suppl):1435–1525.
- Hull CW. Apparatus for production of three-dimensional objects by stereolithography. Google Patents; 1986.
- Gopinathan J, Noh I. Recent trends in bioinks for 3D printing. *Biomater Res*. 2018;22(1):1–15.
- Goole J, Amighi K. 3D printing in pharmaceuticals: a new tool for designing customized drug delivery systems. *Int J Pharm*. 2016;499(1–2):376–94.
- Kang H, Lee SJ, Ko IK, Kengla C, Yoo JJ, Atala A. A 3D bioprinting system to produce human-scale tissue constructs with structural integrity. *Nat Biotechnol*. 2016;34(3):312–9.
- Murphy SV, Atala A. 3D bioprinting of tissues and organs. *Nat Biotechnol*. 2014;32(8):773–85.
- Ventola CL. Medical applications for 3D printing: current and projected uses. *Pharm Ther*. 2014;39(10):704–11.
- Rasperini G, Pilipchuk SP, Flanagan CL, Park CH, Pagni G, Hollister SJ, et al. 3D-printed bioresorbable scaffold for periodontal repair. *J Dent Res*. 2015;94(9_suppl):1535–1575.
- Derby B. Printing and prototyping of tissues and scaffolds. *Science*. 2012;338(6109):921–6.
- Gateno J, Allen ME, Teichgraeber JF, Messersmith ML. An in vitro study of the accuracy of a new protocol for planning distraction osteogenesis of the mandible. *J Oral Maxillofac Surg*. 2000;58(9):985–90.
- D'Urso PS, Barker TM, Earwaker WJ, Bruce LJ, Atkinson RL, Lanigan MW, et al. Stereolithographic biomodelling in cranio-maxillofacial surgery: a prospective trial. *J Craniomaxillofac Surg*. 1999;27(1):30–7.
- Vaquette C, Fan W, Xiao Y, Hamlet S, Huttmacher DW, Ivanovski S. A biphasic scaffold design combined with cell sheet technology for simultaneous regeneration of alveolar bone/periodontal ligament complex. *Biomaterials*. 2012;33(22):5560–73.
- Park CH, Rios HF, Jin Q, Sugai JV, Padial-Molina M, Taut AD, et al. Tissue engineering bone-ligament complexes using fiber-guiding scaffolds. *Biomaterials*. 2012;33(1):137–45.
- Lee CH, Hajibandeh J, Suzuki T, Fan A, Shang P, Mao JJ. Three-dimensional printed multiphase scaffolds for regeneration of periodontium complex. *Tissue Eng Part A*. 2014;20(7–8):1342–51.
- Allan B, Ruan R, Landao-Bassonga E, Gillman N, Wang T, Gao J, et al. Collagen membrane for guided bone regeneration in dental and orthopedic applications. *Tissue Eng Part A*. 2021;27(5–6):372–81.
- Persikov AV, Ramshaw JAM, Kirkpatrick A, Brodsky B. Electrostatic interactions involving lysine make major contributions to collagen triple-helix stability. *Biochemistry*. 2005;44(5):1414–22.
- Sorushanova A, Delgado LM, Wu Z, Shologu N, Kshirsagar A, Raghunath R, et al. The collagen suprafamily: from biosynthesis to advanced biomaterial development. *Adv Mater*. 2019;31(1):e1801651.
- Kuo K, Lin R, Tien H, Wu P, Li Y, Melero-Martin JM, et al. Bioengineering vascularized tissue constructs using an injectable cell-laden enzymatically crosslinked collagen hydrogel derived from dermal extracellular matrix. *Acta Biomater*. 2015;27:151–66.
- Bahney CS, Hsu C, Yoo JU, West JL, Johnstone B. A bioresponsive hydrogel tuned to chondrogenesis of human mesenchymal stem cells. *FASEB J*. 2011;25(5):1486–96.
- Gauza-Włodarczyk M, Kubisz L, Mielcarek S, Włodarczyk D. Comparison of thermal properties of fish collagen and bovine collagen in the temperature range 298–670 K. *Mater Sci Eng C Mater Biol Appl*. 2017;80:468–71.
- Han Y, Hu J, Sun G. Recent advances in skin collagen: functionality and non-medical applications. *J Leather Sci Eng*. 2021;3(1):1–12.
- Yan X, Chen Y, Dan W, Dan N, Li Z. *Bletilla striata* polysaccharide modified collagen fiber composite sponge with rapid hemostasis function. *J Leather Sci Eng*. 2022;4(1):5.
- Chang S, Buehler MJ. Molecular biomechanics of collagen molecules. *Mater Today*. 2014;17(2):70–6.
- Terzi A, Storelli E, Bettini S, Sibillano T, Altamura D, Salvatore L, et al. Effects of processing on structural, mechanical and biological properties of collagen-based substrates for regenerative medicine. *Sci Rep*. 2018;8(1):1429.
- Yu X, Zhang H, Miao Y, Xiong S, Hu Y. Recent strategies of collagen-based biomaterials for cartilage repair: from structure cognition to function endowment. *J Leather Sci Eng*. 2022;4(1):1–23.
- Zhang Y, Trigani KT, Shankar KN, Crossen J, Liu Y, Sinno T, et al. Anti-GPVI Fab reveals distinct roles for GPVI signaling in the first platelet layer and subsequent layers during microfluidic clotting on collagen with or without tissue factor. *Thromb Res*. 2022;218:112–29.
- Kulkarni P, Maniyar M, Nalawade M, Bhagwat P, Pillai S. Isolation, biochemical characterization, and development of a biodegradable antimicrobial film from *Cirrhinus mrigala* scale collagen. *Environ Sci Pollut Res Int*. 2022;29(13):18840–50.
- Chen H, Xue L, Gong G, Pan J, Wang X, Zhang Y, et al. Collagen-based materials in reproductive medicine and engineered reproductive tissues. *J Leather Sci Eng*. 2022;4(1):1–15.
- Coentro JQ, di Nubila A, May U, Prince S, Zwaagstra J, Järvinen TAH, et al. Dual drug delivery collagen vehicles for modulation of skin fibrosis in vitro. *Biomed Mater*. 2022;17(2):25017.
- Chinh NT, Manh VQ, Hoang T, Ramadass K, Sathish CI, Trung VQ, et al. Optimizing the component ratio to develop the biocomposites with carrageenan/collagen/allopurinol for the controlled drug release. *J Drug Deliv Sci Technol*. 2022;68:102697.
- Tang P, Zheng T, Yang C, Li G. Enhanced physicochemical and functional properties of collagen films cross-linked with laccase oxidized phenolic acids for active edible food packaging. *Food Chem*. 2022;393:133353.
- Andreassen RC, Rønning SB, Solberg NT, Grønlien KG, Kristoffersen KA, Høst V, et al. Production of food-grade microcarriers based on by-products from the food industry to facilitate the expansion of bovine skeletal muscle satellite cells for cultured meat production. *Biomaterials*. 2022;286:121602.

39. Lubart R, Yariv I, Fixler D, Lipovsky A. A novel facial cream based on skin-penetrable fibrillar collagen microparticles. *J Clin Aesthet Dermatol.* 2022;15(5):59–64.
40. Agustin EW, Tassabila DEC, Nisa ZA, Rizqi IK, Safitri EN, Sulistiyowati MI. Collagen face spray: facial moisturizer from chicken egg shell membrane to prevent premature aging. *IOP Conf Ser Earth Environ Sci.* 2022;969(1):12008.
41. Igielska-Kalwat J, Kilian-Pięta E, Połoczańska-Godek S. The use of natural collagen obtained from fish waste in hair styling and care. *Polymers.* 2022;14(4):749.
42. Zhang F, Wang C, Mu C, Lin W. A novel hydrophobic all-biomass aerogel reinforced by dialdehyde carboxymethyl cellulose for oil/organic solvent-water separation. *Polymer.* 2022;238:124402.
43. Tan H, Wu B, Li C, Mu C, Li H, Lin W. Collagen cryogel cross-linked by naturally derived dialdehyde carboxymethyl cellulose. *Carbohydr Polym.* 2015;129:17–24.
44. Lee J, Kim G. Collagen-based shape-memory biocomposites. *PAPPL Phys Rev.* 2022;9(2):21415.
45. Xu W, Wu X, Wen Q, Li S, Song Y, Shi B. Effects of collagen fiber addition on the combustion and thermal stability of natural rubber. *J Leather Sci Eng.* 2020;2(1):1–10.
46. Li H, Zheng W, Xiao H, Hao B, Wang Y, Huang X, et al. Collagen fiber membrane-derived chemically and mechanically durable superhydrophobic membrane for high-performance emulsion separation. *J Leather Sci Eng.* 2021;3(1):1–10.
47. Kleinnijenhuis AJ, van Holthoorn FL, van der Steen B. Identification of collagen 1a3 in teleost fish species and typical collagen induced inter-nal fragmentations. *Food Chem X.* 2022;14:100333.
48. Jaziri AA, Shapawi R, Mokhtar RAM, Noordin WNM, Huda N. Biochemical and microstructural properties of lizardfish (*Saurida tumbil*) scale collagen extracted with various organic acids. *Gels.* 2022;8(5):266.
49. Bi C, Li X, Xin Q, Han W, Shi C, Guo R, et al. Effect of extraction methods on the preparation of electrospon/electrosprayed microstructures of tilapia skin collagen. *J Biosci Bioeng.* 2019;128(2):234–40.
50. Chen L, Cheng G, Meng S, Ding Y. Collagen membrane derived from fish scales for application in bone tissue engineering. *Polymers.* 2022;14(13):2532.
51. Blanco M, Sanz N, Sánchez AC, Correa B, Pérez-Martín RI, Sotelo CG. Molecular weight analysis of blue shark (*Prionace glauca*) collagen hydrolysates by GPC-LS; effect of high molecular weight hydrolysates on fibroblast cultures: mRNA collagen type I expression and synthesis. *Int J Mol Sci.* 2022;23(1):32.
52. Ghodbane SA, Dunn MG. Physical and mechanical properties of cross-linked type I collagen scaffolds derived from bovine, porcine, and ovine tendons. *J Biomed Mater Res A.* 2016;104(11):2685–92.
53. González-Masís J, Cubero-Sesin JM, Guerrero S, González-Camacho S, Corrales-Ureña YR, Redondo-Gómez C, et al. Self-assembly study of type I collagen extracted from male Wistar Hannover rat tail tendons. *Biomater Res.* 2020;24(1):1–11.
54. Coppola D, Oliviero M, Vitale GA, Lauritano C, D'Ambra I, Iannace S, et al. Marine collagen from alternative and sustainable sources: extraction, processing and applications. *Mar Drugs.* 2020;18(4):214.
55. Noorzai S, Verbeek CJR, Lay MC, Swan J. Collagen extraction from various waste bovine hide sources. *Waste Biomass Valoriz.* 2020;11(11):5687–98.
56. Ferraro V, Gaillard-Martinie B, Sayd T, Chambon C, Anton M, Santé-Lhoutellier V. Collagen type I from bovine bone. Effect of animal age, bone anatomy and drying methodology on extraction yield, self-assembly, thermal behaviour and electrokinetic potential. *Int J Biol Macromol.* 2017;97:55–66.
57. He L, Lan W, Zhao Y, Chen S, Liu S, Cen L, et al. Characterization of bio-compatible pig skin collagen and application of collagen-based films for enzyme immobilization. *RSC Adv.* 2020;10(12):7170–80.
58. Brodsky B, Eikenberry EF. Characterization of fibrous forms of collagen. In: *Methods enzymology.* 1982, p. 127–74.
59. Campbell PN. Bovine spongiform encephalopathy—some surprises for biochemists. *IUBMB Life.* 2005;57(4–5):273–6.
60. Raman M, Gopakumar K. Fish collagen and its applications in food and pharmaceutical industry: a review. *EC Nutr.* 2018;13(12):752–67.
61. Jaziri AA, Shapawi R, Mokhtar RAM, Noordin WNM, Huda N. Micro-structural and physicochemical analysis of collagens from the skin of lizardfish (*Saurida tumbil* bloch, 1795) extracted with different organic acids. *Molecules.* 2022;27(8):2452.
62. Takeshi N, Nobutaka S, Yasuhiro T, Norihisa K. Collagen from tendon of yezo sika deer (*Cervus nippon yesoensis*) as by-product. *Food Nutr Sci.* 2012;2012:8.
63. Kolodziejska I, Sikorski ZE, Niecikowska C. Parameters affecting the isolation of collagen from squid (*Illex argentinus*) skins. *Food Chem.* 1999;66(2):153–7.
64. Tamilmozhi S, Veeruraj A, Arumugam M. Isolation and characterization of acid and pepsin-solubilized collagen from the skin of sailfish (*Istiophorus platypterus*). *Food Res Int.* 2013;54(2):1499–505.
65. Li C, Song W, Wu J, Lu M, Zhao Q, Fang C, et al. Thermal stable characteristics of acid-and pepsin-soluble collagens from the carapace tissue of Chinese soft-shelled turtle (*Pelodiscus sinensis*). *Tissue Cell.* 2020;67:101424.
66. Park SH, Jo Y. Static hydrothermal processing and fractionation for production of a collagen peptide with anti-oxidative and anti-aging properties. *Process Biochem.* 2019;83:176–82.
67. Indriani S, Benjakul S, Kishimura H, Karnjanapratum S, Nalinanon S. Impact of extraction condition on the yield and molecular characteristics of collagen from Asian bullfrog (*Rana tigerina*) skin. *LWT.* 2022;162:113439.
68. Sorushanova A, Skoufos I, Tzora A, et al. The influence of animal species, gender and tissue on the structural, biophysical, biochemical and biological properties of collagen sponges. *J Mater Sci Mater Med.* 2021;32(1):1–12.
69. Tan Y, Chang SKC. Isolation and characterization of collagen extracted from channel catfish (*Ictalurus punctatus*) skin. *Food Chem.* 2018;242:147–55.
70. Luo Q, Chi C, Yang F, Zhao Y, Wang B. Physicochemical properties of acid-and pepsin-soluble collagens from the cartilage of Siberian sturgeon. *Environ Sci Pollut Res Int.* 2018;25(31):31427–38.
71. Akram AN, Zhang C. Effect of ultrasonication on the yield, functional and physicochemical characteristics of collagen-II from chicken sternal cartilage. *Food Chem.* 2020;307:125544.
72. Li D, Mu C, Cai S, Lin W. Ultrasonic irradiation in the enzymatic extraction of collagen. *Ultrason Sonochem.* 2009;16(5):605–9.
73. Matinong AME, Chisti Y, Pickering KL, Haverkamp RG. Collagen extraction from animal skin. *Biology.* 2022;11(6):905.
74. Abbas AA, Shakir KA, Walsh MK. Functional properties of collagen extracted from catfish (*Silurus triostegus*) waste. *Foods.* 2022;11(5):633.
75. Wu J, Liao W, Zhang J, Chen W. Thermal behavior of collagen crosslinked with tannic acid under microwave heating. *J Therm Anal Calorim.* 2019;135(4):2329–35.
76. Min S, Jo Y, Park SH. Potential application of static hydrothermal processing to produce the protein hydrolysates from porcine skin by-products. *LWT Food Sci Technol.* 2017;83:18–25.
77. Kittiphattanabawon P, Benjakul S, Visessanguan W, Shahidi F. Isolation and characterization of collagen from the cartilages of brownbanded bamboo shark (*Chiloscyllium punctatum*) and blacktip shark (*Carcharhinus limbatus*). *LWT Food Sci Technol.* 2010;43(5):792–800.
78. Lee EH, Chun SY, Lee JN, Yoon BH, Chung J, Han M, et al. Optimized collagen extraction process to obtain high purity and large quantity of collagen from human perirenal adipose tissue. *Biomed Res Int.* 2022;2022:1–15.
79. Cumming MH, Hall B, Hofman K. Isolation and characterisation of major and minor collagens from hyaline cartilage of Hoki (*Macruronus novaezealandiae*). *Mar Drugs.* 2019;17(4):223.
80. Felim J, Chen C, Tsou D, Kuo H, Kong Z. Effect of different collagen on anterior cruciate ligament transection and medial meniscectomy-induced osteoarthritis male rats. *Front Bioeng Biotechnol.* 2022;10:917474.
81. Shaik MI, Asrul Effendi NF, Sarbon NM. Functional properties of sharpnose stingray (*Dasyatis zugei*) skin collagen by ultrasonication extraction as influenced by organic and inorganic acids. *Biocatal Agric Biotechnol.* 2021;35:102103.
82. Wada M, Koremura N, Hasegawa T. Preparation of beta chain dominant collagen of bovine achilles tendon with pepsin. *Nippon Nogeik Kaishi.* 2000;74(7):775–9.

83. Derakhshanfar S, Mbeleck R, Xu K, Zhang X, Zhong W, Xing M. 3D bioprinting for biomedical devices and tissue engineering: a review of recent trends and advances. *Bioact Mater.* 2018;3(2):144–56.
84. Xu HQ, Liu JC, Shahriar M, Xu CX. Investigation of cell aggregation on the printing performance in inkjet-based bioprinting of cell-laden bioink. *Langmuir.* 2023;39(1):545–55.
85. Ozbolat IT, Hospodiuk M. Current advances and future perspectives in extrusion-based bioprinting. *Biomaterials.* 2016;76:321–43.
86. Fatimi A, Okoro OV, Podstawczyk D, Siminska-Stanny J, Shavandi A. Natural hydrogel-based bio-inks for 3D bioprinting in tissue engineering: a review. *Gels.* 2022;8(3):179.
87. Naghieh S, Chen X. Printability—a key issue in extrusion-based bioprinting. *J Pharm Anal.* 2021;11(5):564–79.
88. Garcia-Villen F, Guembe A, Jose MR, Zuniga T, Ruiz-Alonso S, Saenz-Del-Burgo L, et al. Characterization and assessment of new fibrillar collagen inks and bioinks for 3D printing and bioprinting. *Int J Bioprint.* 2023;9(3):712.
89. Kajave NS, Schmitt T, Nguyen TU, Gaharwar AK, Kishore V. Bioglass incorporated methacrylated collagen bioactive ink for 3D printing of bone tissue. *Biomater.* 2021;16(3):035003.
90. Muthusamy S, Kannan S, Lee M, Sanjairaj V, Lu WF, Fuh J, et al. 3D bioprinting and microscale organization of vascularized tissue constructs using collagen-based bioink. *Biotechnol Bioeng.* 2021;118(8):3150–63.
91. Tao O, Kort-Mascort J, Lin Y, Pham HM, Charbonneau AM, ElKashty OA, et al. The applications of 3D printing for craniofacial tissue engineering. *Micromachines.* 2019;10(7):480.
92. Xu T, Binder KW, Albanna MZ, Dice D, Zhao W, Yoo JJ, et al. Hybrid printing of mechanically and biologically improved constructs for cartilage tissue engineering applications. *Biofabrication.* 2013;5(1):15001.
93. Wilson WC, Boland T. Cell and organ printing 1: protein and cell printers. *Anat Rec A Discov Mol Cell Evol Biol.* 2003;272A(2):491–6.
94. Ozbolat IT, Yu Y. Bioprinting toward organ fabrication: challenges and future trends. *IEEE Trans Biomed Eng.* 2013;60(3):691–9.
95. Xu T, Jin J, Gregory C, Hickman JJ, Boland T. Inkjet printing of viable mammalian cells. *Biomaterials.* 2005;26(1):93–9.
96. Vijayavenkataraman S, Yan W, Lu WF, Wang C, Fuh JYH. 3D bioprinting of tissues and organs for regenerative medicine. *Adv Drug Deliv Rev.* 2018;132:296–332.
97. Colosi C, Shin SR, Manoharan V, Massa S, Costantini M, Barbetta A, et al. Microfluidic bioprinting of heterogeneous 3D tissue constructs using low-viscosity bioink. *Adv Mater.* 2016;28(4):677–84.
98. Duan B, Hockaday LA, Kang KH, Butcher JT. 3D Bioprinting of heterogeneous aortic valve conduits with alginate/gelatin hydrogels. *J Biomed Mater Res A.* 2013;101A(5):1255–64.
99. Montalbano G, Calore AR, Vitale Brovarone C. Extrusion 3D printing of a multiphase collagen-based material: an optimized strategy to obtain biomimetic scaffolds with high shape fidelity. *J Appl Polym Sci.* 2023;140(10):e53593.
100. Lee H, Cho DW. One-step fabrication of an organ-on-a-chip with spatial heterogeneity using a 3D bioprinting technology. *Lab Chip.* 2016;16(14):2618–25.
101. Odde DJ, Renn MJ. Laser-guided direct writing for applications in biotechnology. *Trends Biotechnol.* 1999;17(10):385–9.
102. Soman P, Chung PH, Zhang AP, Chen S. Digital microfabrication of user-defined 3D microstructures in cell-laden hydrogels. *Biotechnol Bioeng.* 2013;110(11):3038–47.
103. Mandrycky C, Wang Z, Kim K, Kim D. 3D bioprinting for engineering complex tissues. *Biotechnol Adv.* 2016;34(4):422–34.
104. Duocastella M, Colina M, Fernández-Pradas JM, Serra P, Morenza JL. Study of the laser-induced forward transfer of liquids for laser bioprinting. *Appl Surf Sci.* 2007;253(19):7855–9.
105. Karakaidos P, Kryou C, Simigdala N, Klinakis A, Zergioti I. Laser bioprinting of cells using UV and visible wavelengths: a comparative DNA damage study. *Bioengineering (Basel).* 2022;9(8):378.
106. Keriquel V, Oliveira H, Remy M, Ziane S, Delmond S, Rousseau B, et al. In situ printing of mesenchymal stromal cells, by laser-assisted bioprinting, for in vivo bone regeneration applications. *Sci Rep.* 2017;7(1):1778.
107. Wu Z, Liu J, Lin J, Lu L, Tian J, Li L, et al. Novel digital light processing printing strategy using a collagen-based bioink with prospective cross-linker procyanidins. *Biomacromol.* 2021;23(1):240–52.
108. Xie Z, Shen Z, Zhan P, Yang J, Huang Q, Huang S, et al. Functional dental pulp regeneration: basic research and clinical translation. *Int J Mol Sci.* 2021;22(16):8991.
109. Archibald SJ, Krarup C, Shefner J, Li ST, Madison RD. A collagen-based nerve guide conduit for peripheral nerve repair: an electrophysiological study of nerve regeneration in rodents and nonhuman primates. *J Comp Neurol.* 1991;306(4):685–96.
110. Klein S, Vykoukal J, Felthaus O, Dienstknecht T, Prantl L. Collagen type I conduits for the regeneration of nerve defects. *Materials.* 2016;9(4):219.
111. Lee W, Pinckney J, Lee V, Lee J, Fischer K, Polio S, et al. Three-dimensional bioprinting of rat embryonic neural cells. *NeuroReport.* 2009;20(8):798–803.
112. Chang J, Lin J, Yao C, Chen J, Lai T, Chen Y. In vivo evaluation of a biodegradable EDC/NHS-cross-linked gelatin peripheral nerve guide conduit material. *Macromol Biosci.* 2007;7(4):500–7.
113. Li X, Wang X, Wang X, Chen H, Zhang X, Zhou L, et al. 3D bioprinted rat Schwann cell-laden structures with shape flexibility and enhanced nerve growth factor expression. *3 Biotech.* 2018;8(8):1–10.
114. Liu J, Zhang B, Li L, Yin J, Fu J. Additive-lathe 3D bioprinting of bilayered nerve conduits incorporated with supportive cells. *Bioact Mater.* 2021;6(1):219–29.
115. Song S, Liu X, Huang J, Zhang Z. Neural stem cell-laden 3D bioprinting of polyphenol-doped electroconductive hydrogel scaffolds for enhanced neuronal differentiation. *Biomater Adv.* 2022;133:112639.
116. Hilken P, Bronckaers A, Ratajczak J, Gervois P, Wolfs E, Lambrechts I. The angiogenic potential of DPSCs and SCAPs in an in vivo model of dental pulp regeneration. *Stem Cells Int.* 2017;2017:1–14.
117. Duarte Campos DF, Zhang S, Kreimendahl F, Köpf M, Fischer H, Vogt M, et al. Hand-held bioprinting for de novo vascular formation applicable to dental pulp regeneration. *Connect Tissue Res.* 2020;61(2):205–15.
118. Dixon AR, Jariwala SH, Bilis Z, Loverde JR, Pasquina PF, Alvarez LM. Bridging the gap in peripheral nerve repair with 3D printed and bioprinted conduits. *Biomaterials.* 2018;186:44–63.
119. Yu X, Zhang T, Li Y. 3D printing and bioprinting nerve conduits for neural tissue engineering. *Polymers.* 2020;12(8):1637.
120. Zhang Q, Nguyen PD, Shi S, Burrell JC, Cullen DK, Le AD. 3D bio-printed scaffold-free nerve constructs with human gingiva-derived mesenchymal stem cells promote rat facial nerve regeneration. *Sci Rep.* 2018;8(1):6634.
121. Liu S, Yang H, Chen D, Xie Y, Tai C, Wang L, et al. Three-dimensional bioprinting sodium alginate/gelatin scaffold combined with neural stem cells and oligodendrocytes markedly promoting nerve regeneration after spinal cord injury. *Regen Biomater.* 2022;9:rbac038.
122. Dissanayaka WL, Zhang C. The role of vasculature engineering in dental pulp regeneration. *J Endod.* 2017;43(9):S102–6.
123. Yang M. Regenerative endodontics: a new treatment modality for pulp regeneration. *JSM Dent.* 2013;1(2):10–1.
124. Duarte CD, Zhang S, Kreimendahl F, Köpf M, Fischer H, Vogt M, et al. Hand-held bioprinting for de novo vascular formation applicable to dental pulp regeneration. *Connect Tissue Res.* 2020;61(2):205–15.
125. Emar AA, Shah R. Recent update on craniofacial tissue engineering. *J Tissue Eng.* 2021;12:1758494039.
126. Dwivedi R, Mehrotra D. 3D bioprinting and craniofacial regeneration. *J Oral Biol Craniofac Res.* 2020;10(4):650–9.
127. Rhee S, Puetzer JL, Mason BN, Reinhart-King CA, Bonassar LJ. 3D bioprinting of spatially heterogeneous collagen constructs for cartilage tissue engineering. *ACS Biomater Sci Eng.* 2016;2(10):1800–5.
128. Yang X, Lu Z, Wu H, Li W, Zheng L, Zhao J. Collagen-alginate as bioink for three-dimensional (3D) cell printing based cartilage tissue engineering. *Mater Sci Eng C Mater Biol Appl.* 2018;83:195–201.
129. Fahimipour F, Dashtimoghadam E, Rasouliaboroujeni M, Yazdimaghani M, Khoshroo K, Tahriri M, et al. Collagenous matrix supported by a 3D-printed scaffold for osteogenic differentiation of dental pulp cells. *Dent Mater.* 2018;34(2):209–20.
130. Helgeland E, Mohamed-Ahmed S, Shanbhag S, Pedersen TO, Rosen A, Mustafa K, et al. 3D printed gelatin–genipin scaffolds for temporomandibular joint cartilage regeneration. *Biomed Phys Eng Express.* 2021;7(5):055025.
131. Helgeland E, Rashad A, Campodoni E, Goksoyr O, Pedersen TO, Sandri M, et al. Dual-crosslinked 3D printed gelatin scaffolds with potential

- for temporomandibular joint cartilage regeneration. *Biomed Mater.* 2021;16(3):035026.
132. Nguyen TT, Hu CC, Sakthivel R, Nabilla SC, Huang YW, Yu J, et al. Preparation of gamma poly-glutamic acid/hydroxyapatite/collagen composite as the 3D-printing scaffold for bone tissue engineering. *Biomater Res.* 2022;26(1):21.
 133. Sedghi LM, Bacino M, Kapila YL. Periodontal disease: the good, the bad, and the unknown. *Front Cell Infect Microbiol.* 2021;11:1210.
 134. Xu X, Zhou Y, Zheng K, Li X, Li L, Xu Y. 3D polycaprolactone/gelatin-oriented electrospun scaffolds promote periodontal regeneration. *ACS Appl Mater Interfaces.* 2022;14(41):46145–60.
 135. Wu B, Cheng K, Liu M, Liu J, Jiang D, Ma S, et al. Construction of hyper-elastic model of human periodontal ligament based on collagen fibers distribution. *J Mech Behav Biomed Mater.* 2022;135:105484.
 136. Staples R, Ivanovski S, Vaquette C. Fibre-guiding biphasic scaffold for perpendicular periodontal ligament attachment. *Acta Biomater.* 2022;150:221–37.
 137. Bartold PM, McCulloch CA, Narayanan AS, Pitaru S. Tissue engineering: a new paradigm for periodontal regeneration based on molecular and cell biology. *Periodontol.* 2000;2000(24):253–69.
 138. Yamada S, Shanbhag S, Mustafa K. Scaffolds in periodontal regenerative treatment. *Dent Clin.* 2022;66(1):111–30.
 139. Elango J, Selvaganapathy PR, Lazzari G, Bao B, Wenhui W. Biomimetic collagen-sodium alginate-titanium oxide (TiO₂) 3D matrix supports differentiated periodontal ligament fibroblasts growth for periodontal tissue regeneration. *Int J Biol Macromol.* 2020;163:9–18.
 140. Liu H, Wang C, Sun X, Zhan C, Li Z, Qiu L, et al. Silk fibroin/collagen/hydroxyapatite scaffolds obtained by 3D printing technology and loaded with recombinant human erythropoietin in the reconstruction of alveolar bone defects. *ACS Biomater Sci Eng.* 2022;8(12):5245–56.
 141. Vahdatinia F, Hooshyarfard A, Jamshidi S, Shojaei S, Patel K, Moeinifard E, et al. 3D-printed soft membrane for periodontal guided tissue regeneration. *Materials.* 2023;16(4):1364.
 142. Lin HH, Chao PG, Tai WC, Chang PC. 3D-printed collagen-based waveform microfibrillar scaffold for periodontal ligament reconstruction. *Int J Mol Sci.* 2021;22(14):7725.
 143. Yu M, Luo D, Qiao J, Guo J, He D, Jin S, et al. A hierarchical bilayer architecture for complex tissue regeneration. *Bioact Mater.* 2022;10:93–106.
 144. Pan T, Song W, Xin H, Yu H, Wang H, Ma D, et al. MicroRNA-activated hydrogel scaffold generated by 3D printing accelerates bone regeneration. *Bioact Mater.* 2022;10:1–14.

Publisher's Note

Springer Nature remains neutral with regard to jurisdictional claims in published maps and institutional affiliations.

Submit your manuscript to a SpringerOpen[®] journal and benefit from:

- Convenient online submission
- Rigorous peer review
- Open access: articles freely available online
- High visibility within the field
- Retaining the copyright to your article

Submit your next manuscript at ► [springeropen.com](https://www.springeropen.com)
